



Gender Classification with Low-Power Laser Signals

Nevzat OLGUN^{1*}, İbrahim TÜRKOĞLU²

¹Zonguldak Bulent Ecevit University, Department of Computer Technologies, Zonguldak

²Firat University, Department of Software Engineering, Elazig

Abstract

Gender classification can provide significant advantages in applications with access control, marketing activities and biometric verification processes. In cases where the entries to some areas are only male or female, advertising products according to the number of male and female in the store or reducing the database usage burden by primarily gender discrimination in biometric verification can be given as examples of gender classification practices. Gender classification is a binary classification problem as male or female. In traditional methods, gender classification has been made from facial images. One of the biggest difficulties in gender classification from facial images is that the person's face cannot be kept in a certain position, while other is the difficulties in the imaging stage. The desire of the person to hide herself from the cameras, differences in the face and lighting conditions can be given as examples of the difficulties of the image-based methods. In this study, we propose gender classification with low-power laser beams instead of traditional camera-based method of gender classification. In the experimental study conducted for this purpose, a low-powered laser beam is projected onto the subjects' arm for a short period of time from a distance of 2 m, and laser signals reflected from the subjects' arm are recorded. Laser signals reflected from the arm of subjects are classified according to the LSTM deep learning architecture after data preparation, and the subjects' gender is determined. An average classification success rate of 76.20% was achieved as a result of the gender classification study in which 6 men and 6 women between the ages of 19 and 38 participated. The results show that gender classification can be performed with laser signals. Another advantage of this method is that the arm can be easily positioned at the desired location during the receiving signal from the person's arm.

Keywords: Gender Classification, Laser, LSTM, Sex Classification, Signal Processing

Article Info

Received

05/07/2021

Kabul:

29/07/2021

^{1*} Corresponding author: nevzat.olgun@beun.edu.tr

^{**} Part of this work presented orally at the I. International Conference on Interdisciplinary Applications of Artificial Intelligence (ICIDAAI) 2021.

1 Introduction

In the gender classification process, which is a binary classification problem, classes are male and female. The use of the gender classification process is important in the criminal database, marketing industry, biometric verification processes, and so on [1]. Automatic gender classification provides significant benefits in areas where only women or men can enter. Classification of gender first in the criminal database, which has reached a large size, will greatly reduce the processing load on the database [2]. First, with gender classification, the number of people who will be compared biometric in this large database will decrease significantly, and faster, more accurate results will be obtained. In addition, campaigning on the products according to the weight of the number of men or women in the shopping center, advertising on billboards, highlighting the products that appeal to men or women can cause significant increases in the sales volume of the products. A similar application can be used in human computer interfaces. In such a system, voiceover, character or content can be presented according to the gender of the user.

In most difficult circumstances, it is easy for people to determine the gender of a person in front of them. In computer or machine vision systems, gender detection of people is still a challenging task.

Gender recognition is mostly performed according to the gait model [3,4], facial images [1,5,6], sound [7,8] or other sensors [9]. In the literature, it is seen that gender classification studies are mainly done using cameras. Low resolution, low or high light conditions, blurry images, limited angle images, and inability to capture facial expression are important difficulties in camera-based gender identification procedures. On the other hand, in studies conducted with voice, there is the fact that it is necessary to record especially audio from users. In both types of work done with camera and sound, the issue of privacy can be raised. In addition, seismic sensor studies can be applied in a restricted space and a large number of special sensors must be placed in the place where the application will be made [4].

In studies with sound or camera, the desire of people to hide themselves is one of the biggest challenges of the system. Changing the facial expression of the person using different methods (mask, makeup, etc.) or being in completely dark environments will disable the camera-based systems.

In this study, gender determination with low-power laser beams is recommended instead of gender discrimination made with a camera, which has disadvantages such as privacy, light conditions, and the desire to hide oneself. With the proposed system, laser light was shined on the arm of the subjects at a distance for a very short time and the laser signals reflected from the arm were trained with the deep learning architecture designed after preprocessing. The classification success obtained as a result of the training shows the applicability of the proposed system. Since the camera and sound are not used in the proposed system, there is no privacy problem. In addition, since a system such as seismic sensor is not used, there is no need to place additional sensor array on the ground where the work is performed.

The main contributions of the study can be summarized as follows:

- Gender discrimination can be made with a single low-powered laser beam.
- As far as we know, this study is the first to detect the gender of people remotely and without contact with laser signals.
- In gender identification studies with the camera, low or high ambient light significantly reduces the performance of the system. The proposed system is not affected by ambient light.
- A deep learning architecture is recommended that provides high performance.

Other parts of this article are organized as follows. In the second chapter, previous studies on gender recognition are given. In third chapter, detailed information about LSTM, one of the deep learning models, is given. In the fourth chapter, information about the laser device and experimental setup used in the study is given and the proposed method is mentioned. In the sixth chapter, a general summary of the study is made and a discussion on the results is made.

2 Related works

Various devices are used for gender classification. Some of these are devices that require contact and their practical use does not seem possible. Another type is devices that do not require contact. Some of these devices require an appropriate calibration and some are affected by light conditions. During the use of cameras and microphones, personal data can also be obtained and may affect the deprivation

of the person. Studies on gender recognition are listed below.

Anchal et al. have made gender classification using seismic sensors [4]. In their study, they have examined the sound that male and female subjects made from their feet during walking. For this study, seismic sensors have been placed on the grounds where the experiment was conducted. Bales et al., on the other hand, have made a gender classification using 212 seismic sensors placed on the floor of an intelligent building [9]. These types of studies are systems that require high costs and have installation difficulties. At the same time, such systems operate in a limited area and maintenance costs are high.

Qadri et al. have studied gender discrimination from speech signal [8]. They examined the effects of gender on the signal by extracting features from the sound signals they obtained from the subjects.

In the study of Nixon et al. using a camera, gender classification was made from the behavioral model [10]. In their studies, they argued that women shake their hips while walking and men shake their shoulders, and they suggested that a classification can be made based on these behavioral differences.

Kwon et al. made a gender classification based on skeletal images obtained from the camera [11]. For their study, they obtained walking videos from subjects of different age groups. Based on the idea that men and women have different walking patterns.

On the other hand, Zhang et al. made a gait-based gender classification for automatic gender classification based on the video image obtained from cameras at multiple angles [12]. Do et al. made a gender classifier in which they used gait features from camera images at multiple angles [6]. Russell et al. have made the classification of gender and age groups based on the gait model using convolutional neural networks with images from different angles in the CASIA B database [13].

Nayak et al. have proposed gender classification based on facial images [1]. Dileep et al. have studied age group and gender detection from facial images [14]. In their work, they used artificial neural networks (ANN) as a classifier. Mustafa et al. Used Resnet and CNN to determine gender and age from camera images [5].

3 LSTM: Deep learning model

Being popular in recent years, deep learning is used in several fields such as object recognition [15,16], image segmentation [17], speech recognition [18], machine translation [19], natural language processing [20], drug discovery [21] and in similar fields. Deep learning networks are consisting of different architectures based on their usage areas.

Recurrent neural networks (RNNs) are often used in the processing of sequential data such as video subtitles, genome studies, natural language processing, and time series. The RNN architecture focuses on the relationship between the data in the input sequence given to it. The output of cells in this architecture is used as input in the next process, and the output of each cell depends on the output of the previous cell. Figure 1 shows a simple RNN cell and its expansion. In the figure, RNN cell are represented by A , the inputs by X_t and the outputs by h_t .

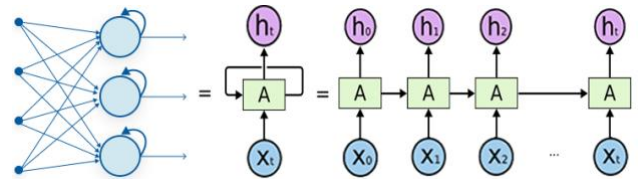


Fig. 1. RNN cell and its expansion

Since RNNs have an internal memory that can also store past information; It can also establish a relationship with the input signal while processing sequential data from sensors over time. While the RNN architecture can successfully establish relationships between short data sequences depending on time, it is unable to establish relationships in long-term data sequences and produce successful results.

The long-term relationship problem in RNN architecture has been solved by Long - Short Term Memory Networks (LSTM) [22]. LSTM consists of a memory cell that can protect its state over time and non-linear gates regulating data input/output in the cell. Input, forget, and output gates in an LSTM cell is interconnected by 4 neural networks and they form the cell memory. LSTM model, gates in its structure as well as the internal structure of an LSTM cell can be seen in Figure 2.

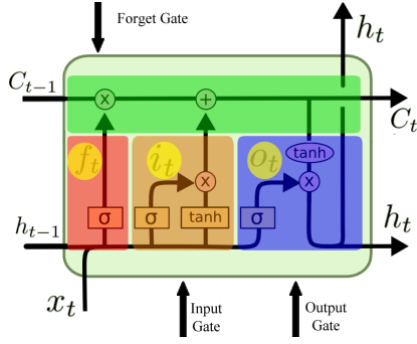


Fig. 2. LSTM model, gates in its structure and the internal structure of the LSTM cell

In LSTM cell model shown in Figure 2, out of the forget gate is represented by f_t , out of the input gate by i_t whereas out of the output gate is represented by o_t , the cell state by C_t and out of the cell by h_t . f_t , i_t , C_t , o_t and h_t are defined in Equations 1, 2, 3, 4, 5. Weights are represented by W_f, W_i, W_c, W_o , bias values are represented by b_f, b_i, b_c, b_o .

$$f_t = \sigma(W_f \cdot [h_{t-1}, x_t] + b_f) \quad (1)$$

$$i_t = \sigma(W_i \cdot [h_{t-1}, x_t] + b_i) \quad (2)$$

$$C_t = f_t * C_{t-1} + i_t * [\tanh(W_c \cdot [h_{t-1}, x_t] + b_c)] \quad (3)$$

$$o_t = \sigma(W_o \cdot [h_{t-1}, x_t] + b_o) \quad (4)$$

$$h_t = o_t * \tanh(C_t) \quad (5)$$

4 Materials and methods

4.1 System design

This study focuses on gender detection from the arm of people, using low-powered laser signals. In the study conducted for this purpose, laser signal reflection on the subjects' arm, recording the signs reflected from the arm, signal preprocessing and classification processes are performed. Figure 3 shows the block diagram of the gender identification study with laser signals.

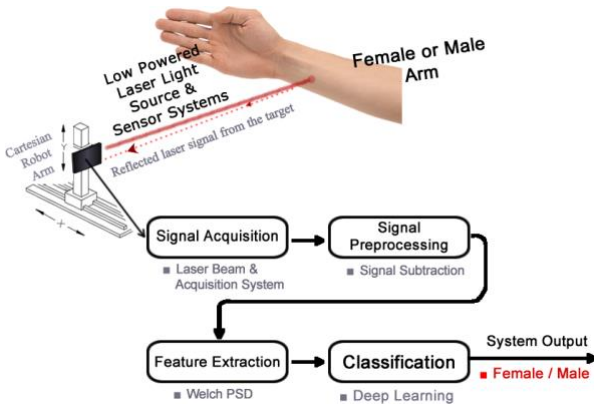


Fig. 3. Gender identification block diagram with low power laser signals

4.2 User selection

Within the scope of the study, laser signals were taken from the arms of 6 healthy men and 6 healthy women. Before starting the experimental study, the users were informed about the laser system and the experimental setup. The age group of users was between 19 and 38. During the sampling, the subjects were asked to place their right hand in the place specified in the experimental setup in a comfortable way.

4.3 Laser beam source and recording system

The laser light source used in the study has an output power of 1mW and a wavelength of 650 nm [23]. The laser light source and recording system used in the study were obtained by reprogramming a laser meter hardware used for distance measurement. The laser module can record a raw laser signal of 3000 points at a sampling frequency of 50 kHz at a time [24,25]. Figure 4 shows the laser module used in the study.

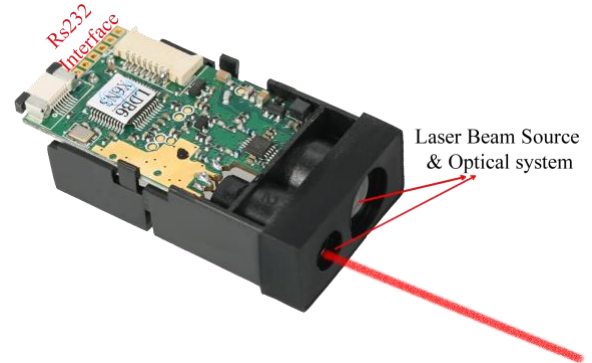


Fig. 4. Laser beam source, optical and recording system

4.4 Experiment setup and data collection procedure

Experimental studies were conducted in a laboratory environment without sunlight and during daylight hours. In the measurements, there is a distance of 2 meters between the laser module and the subjects' arm. Since a large number of sample data is required for deep learning, the laser module was mounted on a Cartesian robot arm moving on the X and Y axis, and 126 laser signals were taken from different points of each subject's arm.

In order to avoid the vibrations caused by the movement of the Robot arm, the measurement was taken 3 seconds after the movement of the arm. For each position, the measurement was taken by reflecting laser light on the subject's arm, and

immediately afterwards, the laser light was turned off and the measurements were made again in order to eliminate the dark current effect caused by the ambient lights and the device. The position of the subjects' arm during the experimental working setup and measurements is shown in Figure 5.



Fig. 5. Experimental working setup and the position of the subjects during the measurement

Starting from the lower right of the subject's arm, measurements were made at 5mm intervals in the pattern order indicated in Figure 6. With the experimental setup, a total of 1512 laser signals were obtained from the arms of male and female subjects. At the same time, when the laser light was turned off, 1512 noise signals created by the dark current and environmental lights of the device were obtained. The motion pattern of the Cartesian robot used to measure laser signals and the arm of the male subject are shown in Figure 6.

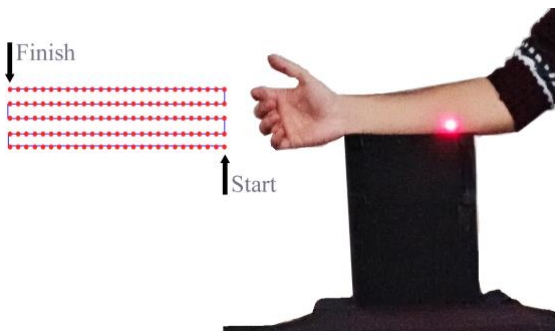


Fig. 6. Movement pattern of the Cartesian robot used to take measurements and the arm of the male subject

4.5 Signal preprocessing steps

In a noisy signal and in cases where the noise is predictably accessible from a separate channel, it may be possible to obtain an estimate of the clean signal by subtracting the estimate of the noise from the noisy signal [26]. In the experimental study for this purpose, the laser signals reflected from the arms of the subjects were recorded when the laser light source was on. Immediately after this process, the laser light source was turned off and the noise signal caused by the device and the ambient light was recorded. Subtraction was used to obtain clear signals from the noisy laser signals obtained from the subjects' arms. Subtraction process was performed to obtain clear signals from the noisy laser signals obtained from the subjects' arms. As stated in Equation 6, from the signals obtained when the laser light source is turned on, the signals obtained when the laser light source is turned off have been subtracted.

$$y(n) = s(n) - d(n) \quad (6)$$

In Equation 6, $y(n)$ refers to the noise-free laser signal, $s(n)$ refers to the noisy laser signal recorded from the subjects' arm, and $d(n)$ refers to the estimated noise generated by the device and environmental lights. Figure 7 shows the laser signal recorded from the female subject's arm while the laser light source was on, the estimated noise signal generated by the device/environmental lights, and the noise-free laser signal obtained as a result of the subtraction process.

4.6 Welch spectral power density and dimension reduction

In this study, the Welch spectral power density of each laser signal obtained after the subtraction process to remove noise from noisy laser signals was calculated. In the Welch method, the size of the raw laser signals was reduced from 3000 to 63 by selecting appropriate parameters. This process also greatly reduces the processing cost for deep learning.

A periodogram is obtained by transforming a signal from time domain to frequency domain. The periodogram used to calculate the spectral power density (PSD) of a time series signal is based on the fast Fourier transform (FFT) [27]. Welch PSD method is based on Barlett method. In the Barlett method, a long signal is divided into multiple windows without overlap, the power spectrum of each window is calculated and spectral density

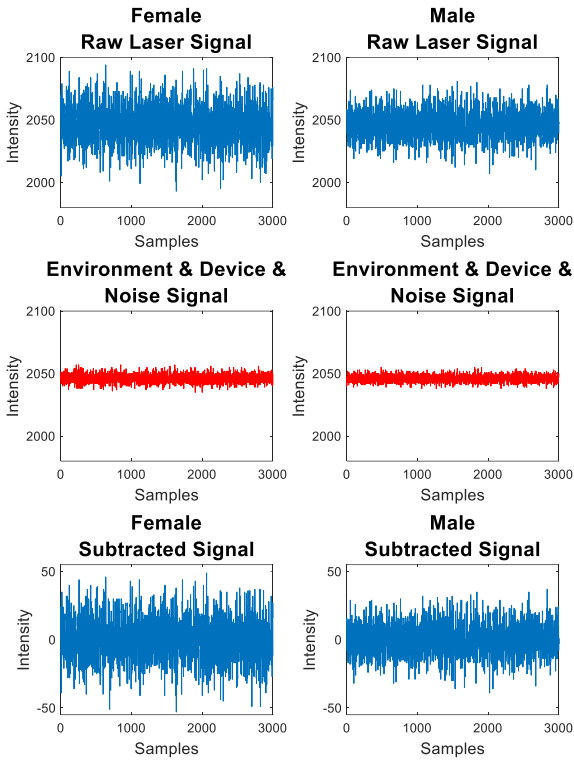


Fig. 7. The noisy laser signal obtained from the arm of the female and male subject, the noise signal measured by turning off the laser light, and the noise-free laser signal obtained as a result of the subtraction process

values are calculated by taking the average of the values at the same frequency. Unlike the Barlett method, in the Welch method, a long signal is divided into windows to overlap and PSD is calculated [28–30]. In the Welch method, the periodogram of a window is calculated in Equation 7 [23].

$$P_l(f) = \frac{1}{M} \frac{1}{P} \left| \sum_{n=1}^M v(n) x_l(n) \exp(-j2\pi f n) \right|^2 \quad (7)$$

In the equation 7, $\{x_l(n), l = 1, \dots, S\}$ represents the windowed segments of the signal, S represents the number of windows, M represents the window length, $v(n)$ represents the windowing function, and $P_l(f)$ represents the periodogram of each windowed segment. According to Welch's method, the periodogram of a signal is calculated as in Equation 8. In the equation, the power distribution of the signal calculated according to the Welch method is represented by $P_w(f)$.

$$P_w(f) = \frac{1}{S} \sum_{l=1}^S P_l(f) \quad (8)$$

In this method, the length of the signal can be calculated with the formula $N = nfft/2 + 1$. In this formula, $nfft$ is a positive value, indicating the number of discrete Fourier transform points to be used in PSD estimation. By taking $nfft = 124$, the size of the laser signal consisting of 3000 points was reduced to 63 points. Figure 8 shows the PSD values of the laser signals of male and female subjects calculated according to the Welch method after subtraction.

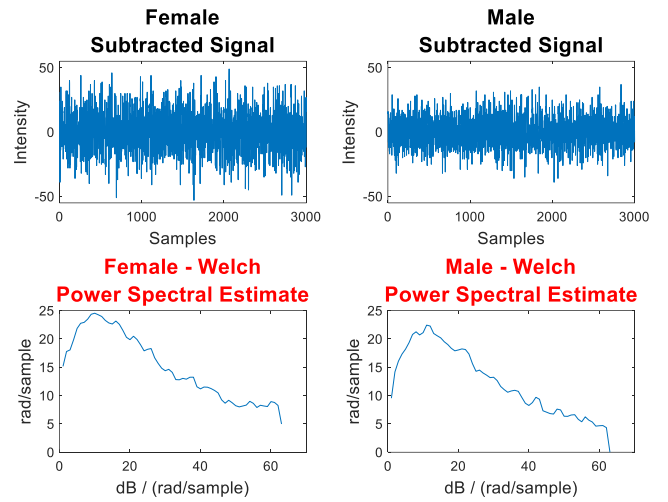


Fig. 8. Pre-processed laser signal and Welch spectral power density signals of male and female subjects

4.7 Deep learning architecture

In this study where gender classification is made from laser signals, the use of the LSTM deep learning model is proposed. The LSTM deep learning model has been the subject of many studies in the field of signal processing and has yielded successful results [31–33]. In the LSTM model, thanks to the memory cell and the forget gate cell in its structure, the relationship between the input and output of the signal can be made and it gives successful results. The LSTM deep learning model proposed in the study and the way signals enter the network is given in Figure 9.

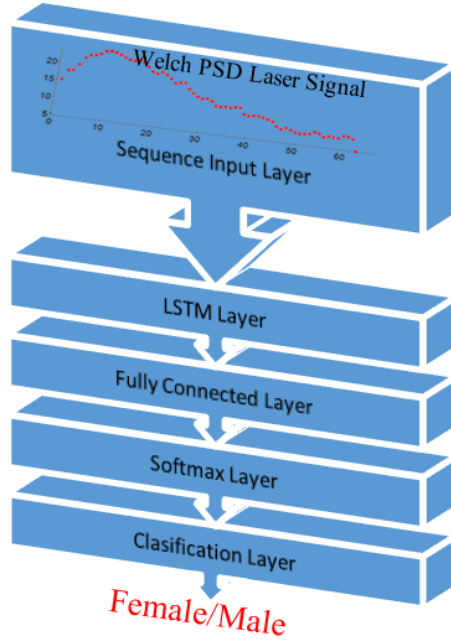


Fig. 9. LSTM model proposed in the study and the way the signal enters the network

In the proposed LSTM model, 63-dimensional PSD values calculated according to the Welch method are used at the input layer. In the model, LSTM layer consisting of 64 hidden units, fully connected layer, SoftMax layer and classification layer are used after the input layer. The LSTM deep learning model proposed in the study is given in Table 1.

Table 1. Layer type and properties used for the LSTM deep learning model.

Layer Number	Layer Type	Properties
Layer 1	Sequence input layer	Sequence input with 63 points
Layer 2	LSTM layer	LSTM with 64 hidden units
Layer 3	Fully connected layer	2 units
Layer 4	Softmax layer	Softmax activation function
Layer 5	Classification output layer	2 classes

For the LSTM model used in the study, hyperparameters are given in Table 2.

Table 2. Hyperparameters of the LSTM model.

Parameter	Type or Value
Optimizer	Adam
Activation	Softmax
Batch Size	512
Max Epochs	1500
Train and Validation Data	90% and 10% of total data

5 Results

In the study, cross-validation technique was used for performance evaluation of the LSTM model. For this purpose, the data set was randomly divided into 10 equal parts, 1 part was excluded for validation at each time, and the remaining 9 parts were used to train the model. The average performance values of the system were calculated by taking the average of the values obtained as a result of each training and validation process. Recall, precision, F1-score and accuracy values were used in performance evaluations. Table 3 shows the average performance evaluation results of the system.

Table 3. Performance values of the system.

Parameter	Rate (%)
Recall	76.163
Precision	75.874
F1-Score	76.018
Accuracy	76,2

The accuracy graph and confusion matrix of the data set with the highest verification as a result of the trainings made with the LSTM model can be seen in Figure 10. The accuracy value in this step was measured as 79.33%. When the confusion matrix is examined, it is seen that 78.2% of female and 79.3% of male are classified correctly. As a result of the training, the lowest accuracy rate was 69.91%.

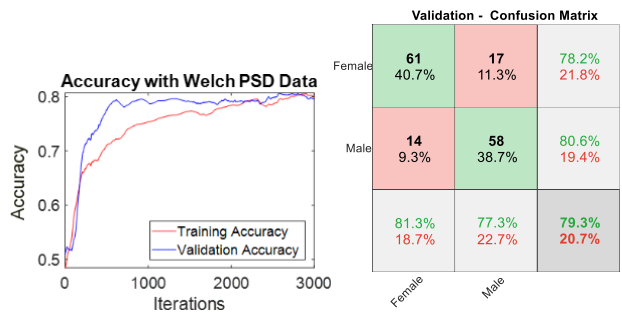


Fig. 10. Accuracy graph and confusion matrix with the highest performance in the study

In the study, the average training and validation time took 268 seconds (4 minutes 28 seconds) for 1512 sample signals. In this case, training and validation time will take approximately 0.18 seconds for a signal. These values show that real-time applications can also be developed.

As far as we know, there is no gender classification study with low-power laser signals in the literature. For this reason, the performance comparison of the system could not be made.

6 Conclusion

In this study, it is proposed to classify the gender from the laser marks reflected from the subjects' arm by projecting laser lights on the subjects' arm at a distance of 2 meters. In the proposed system, PSD values are calculated according to the Welch method from large-sized raw laser signals, their dimensions are reduced and classification is made using the LSTM deep learning model. In the performance evaluation studies using the cross-validation technique, it has been seen that the average performance of the system has been 76.2%. The results obtained show that gender classification can be made with laser signals.

Experimental studies have shown that the training and verification time for a laser signal is approximately 0.2 seconds. Considering these working periods, after training with the deep learning architecture, a learning transfer can be made and a low-capacity microcontroller system can also be used for gender classification with laser signals. In this way, a portable system can be developed.

In future studies, the success of the system in different atmospheric conditions can be studied and the effect of factors such as sun, humidity and rain on the system can be examined. As the distance between the laser system and the subjects change, the intensity of the laser signals reflected from the subjects will also change. With a future study, a system that takes into account the distance between the laser and the subjects can be developed during the decision-making process.

Ethics statements

This study has been done with the approval of Firat University Ethics Committee dated 09.08.2019 and numbered 342810.

Declaration of interests

All authors declare no conflicts of interest in relation to this work.

Acknowledgements

We would like to thank all the participants who participated in this work.

References

- [1] Nayak JS, Indiramma M. An approach to enhance age invariant face recognition performance based on gender classification. *Journal of King Saud University - Computer and Information Sciences* 2021. <https://doi.org/10.1016/j.jksuci.2021.01.005>.
- [2] Juefei-Xu F, Verma E, Savvides M. Deepgender2: A generative approach toward occlusion and low-resolution robust facial gender classification via progressively trained attention shift convolutional neural networks (PTAS-CNN) and deep convolutional generative adversarial networks (DCGAN). *Advances in Computer Vision and Pattern Recognition*, vol. PartF1, Springer London; 2017, p. 183–218. https://doi.org/10.1007/978-3-319-61657-5_8.
- [3] Ali S, Wu Z, Zhou M, Du G, Li X, Pengcheng F. Human identification using sensors data based on 3D gait area. *Proceedings - 2014 International Conference on Cyberworlds, CW 2014*, Institute of Electrical and Electronics Engineers Inc.; 2014, p. 285–92. <https://doi.org/10.1109/CW.2014.46>.
- [4] Anchal S, Mukhopadhyay B, Kar S. Predicting gender from footfalls using a seismic sensor. *2017 9th International Conference on Communication Systems and Networks, COMSNETS 2017*, Institute of Electrical and Electronics Engineers Inc.; 2017, p. 47–54. <https://doi.org/10.1109/COMSNETS.2017.7945357>.
- [5] Mustafa A, Meehan K. Gender Classification and Age Prediction using CNN and ResNet in Real-Time. *2020 International Conference on Data Analytics for Business and Industry: Way Towards a Sustainable Economy, ICDABI 2020*, Institute of Electrical and Electronics Engineers Inc.; 2020, p. 1–6. <https://doi.org/10.1109/ICDABI51230.2020.9325696>.
- [6] Do TD, Nguyen VH, Kim H. Real-time and robust multiple-view gender classification using gait features in video surveillance. *Pattern Analysis and Applications* 2020;23:399–413. <https://doi.org/10.1007/s10044-019-00802-6>.
- [7] Sengupta S, Yasmin G, Ghosal A. Classification of male and female speech using perceptual features. *8th International Conference on Computing, Communications and Networking Technologies, ICCCNT 2017*, Institute of Electrical and Electronics Engineers Inc.; 2017, p. 1–7. <https://doi.org/10.1109/ICCCNT.2017.8204065>.
- [8] Qadri SAA, Gunawan TS, Wani T, Alghifari MF, Mansor H, Kartiwi M. Comparative Analysis of Gender Identification using Speech Analysis and Higher Order Statistics. *2019 IEEE 6th International Conference on Smart Instrumentation, Measurement and Application, ICSIMA 2019*,

- Institute of Electrical and Electronics Engineers Inc.; 2019, p. 1–6.
<https://doi.org/10.1109/ICSIMA47653.2019.9057296>.
- [9] Bales D, Tarazaga PA, Kasarda M, Batra D, Woolard AG, Poston JD, et al. Gender Classification of Walkers via Underfloor Accelerometer Measurements. *IEEE Internet of Things Journal* 2016;3:1259–66.
<https://doi.org/10.1109/JIOT.2016.2582723>.
- [10] Nixon MS, Carter JN. Automatic recognition by gait. *Proceedings of the IEEE* 2006;94:2013–24.
<https://doi.org/10.1109/PROC.2006.886018>.
- [11] Kwon B, Lee S. Joint Swing Energy for Skeleton-Based Gender Classification. *IEEE Access* 2021;9:28334–48.
<https://doi.org/10.1109/ACCESS.2021.3058745>.
- [12] Zhang D, Wang Y. Using multiple views for gait-based gender classification. 26th Chinese Control and Decision Conference, CCDC 2014, IEEE Computer Society; 2014, p. 2194–7.
<https://doi.org/10.1109/CCDC.2014.6852532>.
- [13] Russel NS, Selvaraj A. Gender discrimination, age group classification and carried object recognition from gait energy image using fusion of parallel convolutional neural network. *IET Image Processing* 2021;15:239–51.
<https://doi.org/10.1049/ipr2.12024>.
- [14] Dileep MR, Danti A. Human Age and Gender Prediction Based on Neural Networks and Three Sigma Control Limits. *Applied Artificial Intelligence* 2018;32:281–92.
<https://doi.org/10.1080/08839514.2018.1451217>.
- [15] Pathak AR, Pandey M, Rautaray S. Application of Deep Learning for Object Detection. *Procedia Computer Science*, vol. 132, 2018, p. 1706–17.
<https://doi.org/10.1016/j.procs.2018.05.144>.
- [16] Doğan F, Türkoğlu İ. Derin öğrenme algoritmalarının yaprak sınıflandırma başarımlarının karşılaştırılması. *Sakarya University Journal of Computer and Information Sciences* 2018;1:10–21.
- [17] Betül A, Gurses OA, Oktay AB, Gurses A. Automatic Detection, Localization and Segmentation of Nano-Particles with Deep Learning in Microscopy Images. *Micron* 2019;120:113–9.
<https://doi.org/10.1016/j.micron.2019.02.009>.
- [18] Wang D, Chen J. Supervised speech separation based on deep learning: An overview. *IEEE/ACM Transactions on Audio Speech and Language Processing* 2018.
<https://doi.org/10.1109/TASLP.2018.2842159>.
- [19] Peris Á, Casacuberta F. Online learning for effort reduction in interactive neural machine translation. *Computer Speech and Language* 2019.
<https://doi.org/10.1016/j.csl.2019.04.001>.
- [20] Chatterjee A, Gupta U, Chinnakotla MK, Srikanth R, Galley M, Agrawal P. Understanding Emotions in Text Using Deep Learning and Big Data. *Computers in Human Behavior* 2019.
<https://doi.org/10.1016/j.chb.2018.12.029>.
- [21] Chen H, Engkvist O, Wang Y, Olivecrona M, Blaschke T. The rise of deep learning in drug discovery. *Drug Discovery Today* 2018.
<https://doi.org/10.1016/j.drudis.2018.01.039>.
- [22] Greff K, Srivastava RK, Koutnik J, Steunebrink BR, Schmidhuber J. LSTM: A Search Space Odyssey. *IEEE Transactions on Neural Networks and Learning Systems* 2017;28:2222–32.
<https://doi.org/10.1109/TNNLS.2016.2582924>.
- [23] Olgun N, Türkoğlu İ. Classification of Live/Lifeless Assets with Laser Beams in Different Humidity Environments. 8th International Symposium on Digital Forensics and Security, ISDFS 2020, 2020.
<https://doi.org/10.1109/ISDFS49300.2020.9116314>.
- [24] Olgun N, Türkoğlu İ. Lazer İşaretleri ile Otomatik Hedef Tanıma. *Sak Univ J Comput Inf Sci* 2018;1:1–10.
- [25] Olgun N, Türkoğlu İ. Defining Objects with Laser from a Long Distance via Deep Learning Networks. 10th International Symposium on Intelligent Manufacturing and Service Systems (IMSS'19), Sakarya, Turkey: 2019, p. 1401–11.
- [26] Vaseghi S v. *Advanced Digital Signal Processing and Noise Reduction*. Chichester, UK: John Wiley & Sons, Ltd; 2001. <https://doi.org/10.1002/0470841621>.
- [27] Buttkus B. Estimation of the Power Spectral Density Function. *Spectral Analysis and Filter Theory in Applied Geophysics*, Springer Berlin Heidelberg; 2000, p. 179–213. https://doi.org/10.1007/978-3-642-57016-2_10.
- [28] Kang C, Zhang X, Zhang A, Lin H. Underwater acoustic targets classification using welch spectrum estimation and neural networks. *Lecture Notes in Computer Science (Including Subseries Lecture Notes in Artificial Intelligence and Lecture Notes in Bioinformatics)* 2004;3173:930–5.
https://doi.org/10.1007/978-3-540-28647-9_153.
- [29] Balasaraswathy N, Rajavel R. Low-complexity power spectral density estimation. *Advances in Intelligent Systems and Computing*, vol. 325, Springer Verlag; 2015, p. 273–82. https://doi.org/10.1007/978-81-322-2135-7_30.
- [30] Alkan A, Kiyimik MK. Comparison of AR and Welch methods in epileptic seizure detection. *Journal of Medical Systems* 2006;30:413–9.
<https://doi.org/10.1007/s10916-005-9001-0>.
- [31] Yildirim Ö. A novel wavelet sequences based on deep bidirectional LSTM network model for ECG signal classification. *Computers in Biology and Medicine* 2018;96:189–202.
<https://doi.org/10.1016/j.combiomed.2018.03.016>.
- [32] Michielli N, Acharya UR, Molinari F. Cascaded LSTM recurrent neural network for automated sleep stage classification using single-channel EEG signals.

- Computers in Biology and Medicine 2019;106:71-81.
<https://doi.org/10.1016/j.compbimed.2019.01.013>.
- [33] Garg A, Kapoor A, Bedi AK, Sunkaria RK. Merged LSTM Model for emotion classification using EEG signals. 2019 International Conference on Data Science and Engineering, ICDSE 2019, Institute of Electrical and Electronics Engineers Inc.; 2019, p. 139-43.
<https://doi.org/10.1109/ICDSE47409.2019.8971484>.